

https://doi.org/10.1070/QEL17501

Dynamics of a *Q*-switched bismuth-doped fibre laser: simulation and comparison with experiment

D.E. Artemov, O.E. Nanii, A.P. Smirnov, A.I. Fedoseev

Abstract. **Using an improved travelling wave model, we have numerically investigated the dynamics of a *Q*-switched bismuth-doped fibre laser. Comparison of simulation results with previously reported experimental data demonstrates good agreement of the multipeak lasing structure and the shape of the strongest pulses at various levels of pumping. We have assessed the effect of the main laser parameters on output laser characteristics and quantitatively evaluated the effects of the nonsaturable loss in the active fibre and amplified spontaneous emission on output power saturation. Based on analysis of time-dependent light intensity and gain distributions in the gain medium at different instants in time, we have formulated recommendations how to improve output laser characteristics.**

Keywords: *dynamics of lasing, Q-switching, fibre laser, bismuth.*

1. Introduction

In recent years, bismuth-doped fibre lasers have been the subject of intense research. Characteristic features of such lasers are high efficiency of bismuth-doped active fibre and a broad emission spectrum. Bismuth-doped aluminosilicate, phosphosilicate, and germanosilicate active fibres have a few broad luminescence bands, which enables lasing in the range 1.15–1.75 μm [1, 2]. Of particular research interest are bismuth fibre lasers operating in the wavelength range 1.2–1.3 μm, which is not covered by rare-earth-doped fibre lasers [2]. Most studies so far have addressed cw and mode-locked operation of bismuth fibre lasers [2–6], whereas there has been less work on *Q*-switched operation of bismuth fibre lasers, even though many such studies have been reported for other fibre lasers [7–11]. Only a few experimental studies concerned with *Q*-switched bismuth fibre lasers have been reported to date [12–14], and only Khegai et al. [14] experimentally investigated actively *Q*-switched operation of a bismuth-doped phosphosilicate fibre laser emitting at a wavelength of 1.33 μm. In our opinion, they used a very advantageous experimental configuration for *Q*-switching: two-side-pumped ring laser with minimised spontaneous emission.

D.E. Artemov, O.E. Nanii, A.I. Fedoseev Faculty of Physics, Lomonosov Moscow State University, Vorob'evy gory, 119991 Moscow, Russia; e-mail: artemovdima13@gmail.com;
A.P. Smirnov Faculty of Computational Mathematics and Cybernetics, Lomonosov Moscow State University, Vorob'evy gory, 119991 Moscow, Russia

Received 7 December 2020
Kvantovaya Elektronika **51** (4) 299–305 (2021)
Translated by O.M. Tsarev

The objectives of this work are to gain insight into the key features of the operation of such a laser using an adequate numerical model, compare simulation results with experimental data, and make recommendations on how to improve performance characteristics of the laser.

2. Model laser

The gain medium of the ring laser [14] consists of two pieces of active fibre, which are pumped on opposite sides. Unidirectional lasing is ensured by an optical isolator. An acousto-optic modulator (AOM) located between the two fibre sections is used as a *Q*-switch. This configuration is attractive in that, when the modulator is closed, there is rather low level of amplified spontaneous emission (ASE), which otherwise may reduce *Q*-switched operation efficiency. When closed, the modulator transmits neither spontaneous emission (1.33 μm range) nor pump light (~1.23 μm). When open, the modulator has a spontaneous emission attenuation coefficient of 0.9 and does not transmit pump light. (Details of the experiment can be found in Ref. [14]).

Figure 1 shows a schematic of the laser. The total length of the two fibre sections is $L = L_1 + L_2$. At the output of the second fibre section (coordinate $x = L$), there are an optical isolator and wavelength-selective output coupler. Since the laser cavity length is $L = 100$ m, the sizes of the AOM, isolator, and mirror can be neglected. In this configuration, a light wave reflected from the selective mirror at the $x = L$ point arrives at the $x = 0$ point (shown by a dashed line in the schematic). The pump beam is split into two parts (light at the $x = 0$ and $x = L$ points), which propagate in opposite directions.

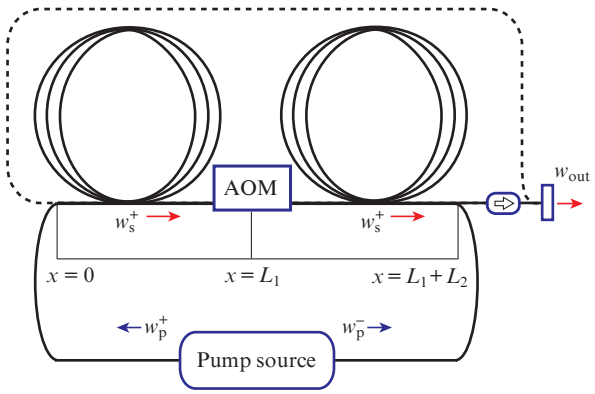

Figure 1. Schematic of the model laser.

It is worth noting that, when the modulator is open, a light wave diffracted from a travelling acoustic wave and, accordingly, frequency-shifted is transmitted through it to the amplifier. The frequency shift on each cavity pass prevents mode structure formation, so the laser is modeless [15, 16].

Amplified spontaneous emission conversion in the laser under consideration has a number of distinctive features. ASE waves in the gain medium can be described by formally representing them as two components differing in spectral bandwidth. One component is narrow (its bandwidth corresponds to the reflection bandwidth of the selective mirror) and the other is broad (its bandwidth is of the order of the gain bandwidth). Only one narrow-band ASE wave, of intensity w_s^+, partially reflected from the mirror, provides feedback in the ring cavity. The broadband wave of intensity v_a^+ is not reflected from the mirror, and the broadband wave of intensity v_a^- is not transmitted by the optical isolator. The intensity ratio of the ASE waves in our model is taken to be roughly equal to the ratio of their spectral bandwidths. This is strictly so only for a purely Gaussian (or rectangular) gain profile, but a more accurate relation is difficult to obtain because there are no accurate data on the shape of the spectrum of bismuth active centres (BACs).

It is easy to see that, from the viewpoint of competition between the waves, the conditions that develop when the modulator is open are favourable for the signal wave of intensity w_s^+. This wave is amplified considerably more rapidly owing to the feedback and saturates the medium, resulting in unidirectional lasing. In the interval [0, L_1], where the light reflected from the mirror arrives, the intensity w_s^+ in the case of a positive gain is always lower than that in the interval [L_1, L]. This type of intensity distribution allows the [0, L_1] section of the gain medium to be formally referred to as an oscillator, and the [L_1, L] section, as an amplifier.

3. Model and equations

For the pump process chosen [14], the gain medium is represented by a quasi-two-level model. For the pump (λ = 1.23 μm), signal, and ASE (λ =1.33 μm) fields, the transport equation approximation is used in calculations (see e.g. Refs [7–10]). Equations for the pump ($w_p^\pm$), signal (w_s^+), and ASE ($v_a^\pm$) intensities take into account nonsaturable losses at the corresponding wavelengths. The numerical model assumes that the pump, signal, and broadband ASE fields change the population of the upper laser level of BACs. The relaxation time of this level, T_{10}, is thought to be roughly constant and independent of the degree and mechanism of its excitation. We found no published data on possible variations in the relaxation time of BACs.

For normalised quantities, the equations and boundary conditions have the form

$$\frac{\partial w_p^\pm(x,\tau)}{\partial\tau} \pm \frac{\partial w_p^\pm(x,\tau)}{\partial x} = -[\gamma n_0(x,\tau) - \delta n_1(x,\tau) + L\theta_p] w_p^\pm(x,\tau), \quad (1)$$

$$\frac{\partial w_s^+(x,\tau)}{\partial\tau} + \frac{\partial w_s^+(x,\tau)}{\partial x} = [n_1(x,\tau) - \nu n_0(x,\tau) - L\theta_s] w_s^+(x,\tau) + k_s \frac{\Delta\Omega}{4\pi}\xi n_1, \quad (2)$$

$$\frac{\partial v_a^\pm(x,\tau)}{\partial\tau} \pm \frac{\partial v_a^\pm(x,\tau)}{\partial x} = [n_1(x,\tau) - \nu n_0(x,\tau) - L\theta_s] v_s^\pm(x,\tau) + \frac{\Delta\Omega}{4\pi}\xi n_1, \quad (3)$$

$$\frac{\partial n_1(x,\tau)}{\partial\tau} = -\xi n_1(x,\tau) - [n_1(x,\tau) - \nu n_0(x,\tau)] w(x,\tau) + [n_0(x,\tau) - \mu n_1(x,\tau)] w_p(x,\tau), \quad (4)$$

$$n = n_0(x,\tau) + n_1(x,\tau), \quad (5)$$

$$w_s^+(0,\tau) = R w_s^+(1,\tau),\ v_a^-(1,\tau) = 0,\ v_a^+(0,\tau) = 0,\quad w_{out} = (1-R) w_s^+(1,\tau),\ w_p^\pm(0.5,\tau) = 0. \quad (6)$$

Here, τ is the time normalised to the gain medium (cavity) single-pass time, T_c; x is the coordinate normalised to the gain medium length, L; $w_p^\pm = T_c\sigma_{ap} I_p^\pm/(h\nu_p)$ (where $I_p^\pm$ is the dimensional pump intensity; σ_{ap} is the absorption cross section at the pump wavelength; and $h\nu_p$ is the pump photon energy); $w_s^\pm = T_c\sigma_{es} I_s^\pm/(h\nu_s)$ (where $I_s^\pm$ is the dimensional signal intensity; σ_{es} is the stimulated emission cross section at the signal wavelength; and $h\nu_s$ is the signal photon energy); $v_a^\pm = T_c\sigma_{es} I_a^\pm/(h\nu_s)$ (where $I_a^\pm$ is the dimensional broadband ASE intensity in the corresponding direction); $w_p = w_p^+ + w_p^-$; $w = w_s^+ + v_a^+ + v_a^-$; $n = L\sigma_{es}N$ is a dimensionless BAC concentration (where N is the dimensional BAC concentration); $n_0(x,\tau)$ and $n_1(x,\tau)$ are dimensionless populations of the lower and upper laser levels, expressed through the corresponding dimensional populations, like in the case of the dimensionless BAC concentration; θ_p and θ_s are the dimensional nonsaturable losses at the pump and signal wavelengths, respectively; the $\Delta\Omega/4\pi$ ratio determines the solid angle subtended by the spontaneous emission propagating in the fibre; the coefficient k_s determines the fraction of ASE involved in lasing and is the ratio of the reflection bandwidth of the mirror to the gain bandwidth; R is the reflectivity of the mirror; $\xi = T_c/T_{10}$; $\gamma = \sigma_{ap}/\sigma_{es}$; $\delta = \sigma_{ep}/\sigma_{es}$; $\nu = \sigma_{as}/\sigma_{es}$; and $\mu = \sigma_{ep}/\sigma_{ap}$ (where σ_{ep} is the stimulated emission cross section at the pump wavelength and σ_{as} is the absorption cross section at the signal wavelength).

The numerical values of the main parameters were taken equal or similar to those given in Ref. [14]: T_{10} = 700 μs, $n = 4.1\times10^{16}$ cm^{-3}, $\sigma_{ap} = 2.4\times10^{-20}$ cm^2, $\sigma_{ep} = 0.34\times10^{-20}$ cm^2, $\sigma_{as} = 1.5\times10^{-20}$ cm^2, and $\sigma_{es} = 1.6\times10^{-20}$ cm^2. The nonsaturable losses at the pump and signal wavelengths were $\theta_p = 1.29\times10^{-4}$ cm^{-1} and $\theta_s = 5.76\times10^{-5}$ cm^{-1} [14]. For spontaneous emission, we estimated $\Delta\Omega/(4\pi) = 10^{-4}$ and $k_s = 10^{-2}$. In most calculations, we took R = 0.1 and $L_1 = L_2$ = 120 m.

4. Comparison of the calculation results and experimental data

Figure 2 shows the calculated output power of the laser at various total pump powers launched into the two sections of the active fibre. The modulator is periodically turned on for

~15 μs at a frequency of 500 Hz. The calculations were made for $L_1 = L_2 = 120$ m and several pump powers. Time zero is the instant at which the modulator is opened, and the time scale uses normalised units. Here and in what follows, the variation in the quality factor was modelled by a smooth exponential curve with a characteristic rise time of ~20 ns.

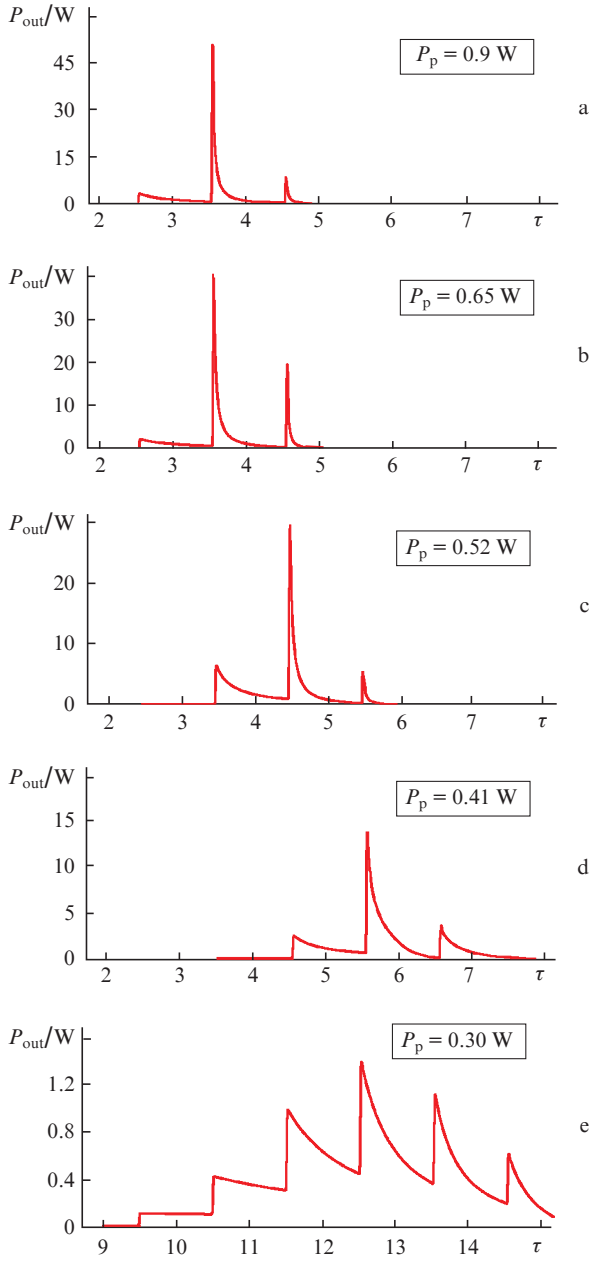

Figure 2. Output laser pulses at different pump powers.

On the whole, the time dependences of the output power agree rather well with experimental data [14]. They have the form of a few pulses forming a spike structure. The pump power influences the time delay of the entire structure relative to the instant at which the modulator is turned on and also the power distribution between individual pulses. The shape of the laser pulses leads us to assume that appreciable saturation of the laser transition occurs only after the last pulse.

The numerical scheme used in our calculations allows for clear interpretation of results because normalised variables meet the relation $\Delta x = \Delta\tau$. Clearly, the formation of the first pulse from the narrow-band spontaneous emission component begins directly after the modulator, located in the middle of the gain medium, is opened. Because of this, the pulse is formed before a detectable level is reached, in a half-integer time τ. The delay corresponding to the pulse formation time increases with decreasing pump power. It is seen from Fig. 2 that the time delay of the first pulse is $\tau = 3.5–9.5$, depending on P_p.

At a relatively low pump power, the structure has a different shape (Fig. 2e). In general terms, the reason for this is that an individual pulse causes only a slight decrease in inversion, its relatively low intensity decreases slowly, and it has an increased width, so the next pulse begins before it ends. The detailed physics underlying the formation of the spike lasing structure is discussed in the next section, where we consider the dynamics of the intensity and gain distributions along the length of the active medium.

Since ASE plays a key role in the laser under consideration, it is of interest to assess the effect of initial spontaneous emission intensity on the amplitude and shape of output pulses. Figure 3 shows calculation results obtained at a varied coefficient k_s (within the model used) and a constant pump power $P_p = 0.52$ W. The coefficient is indicated at the right of each panel. It is seen that even considerable changes in k_s have little effect on the pulse amplitude and shape. At the same time, increasing the intensity of the spontaneous emission involved in laser signal formation reduces the time delay of output pulses, as would be expected. In a number of calculations, we took into account the stochastic character of spontaneous emission at $k_s = 10^{-1}$. To this end, a Langevin factor ranging in amplitude from zero to unity was added to the last term in Eqns (2) and (3). The frequency of changes roughly corresponded to the inverse of the photon lifetime in the gain medium: $\sim 10^8$ s^{-1}. Spontaneous emission stochastisation was found to have a rather weak effect on the pulse position and shape. Figure 4 shows the most intense pulses generated at a pump power of 0.9 W. It is seen that, in the former case (lasing originates from continuous spontaneous emission), the pulse, of duration ~20 ns, is rather smooth, and its edge width is close to the instant when the modulator was opened. In the latter case, there is an insignificant delay and slight distortions of the pulse shape. The discrepancy between the pulse width and the experimentally measured one (~80 ns) can be accounted for by the slower switching-on of the modulator in the experiment. It is also possible that the intensities of different spectral components of the light being amplified grow at different rates, which leads to pulse edge broadening.

Increasing the pump power leads to saturation of the total pulse energy E_{out}. The shape of the calculated curve (Fig. 5) agrees well with experimental data. At the same time, the absolute energy values are about 30% lower than the experimentally determined ones. Calculations demonstrate that, in the range of pump powers under consideration, the intensity of counterpropagating waves of broadband ASE has no

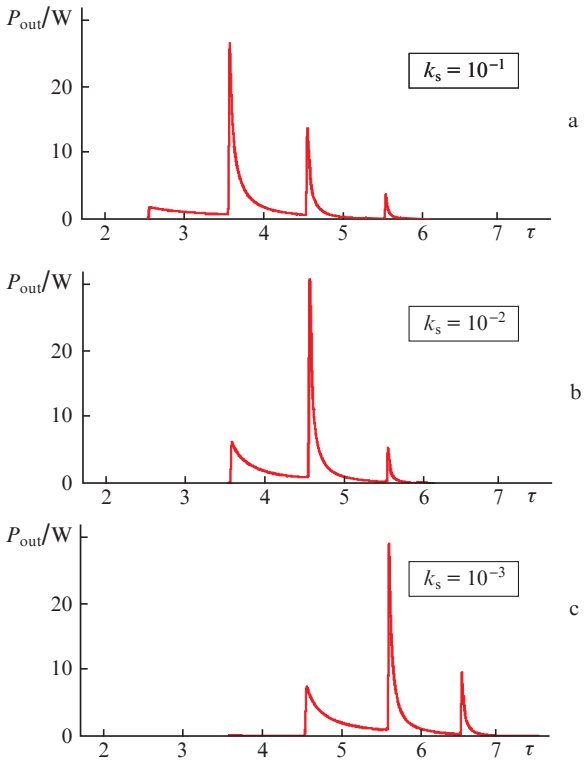

Figure 3. Output laser pulses at different levels of spontaneous emission.

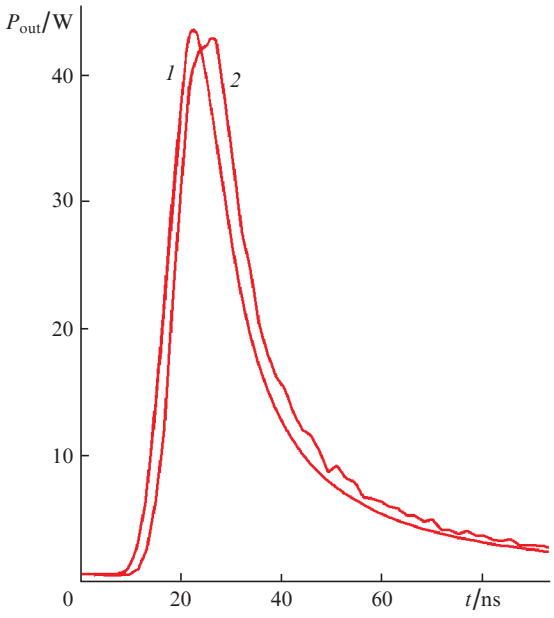

Figure 4. Laser pulses resulting from (*1*) continuous and (*2*) stochastic spontaneous emission at a pump power of 0.9 W.

noticeable effect on E_{out} because, at the instant when lasing begins, the maximum values of v_a^+ and v_a^- are more than four orders of magnitude lower than the pulse amplitude (the data in Fig. 3 also confirm that ASE has a weak effect). The quantitative effect of the nonsaturable loss θ_s at $P_p = 1$ W reduces to the following: As θ_s decreases by a factor of 3, E_{out} increases, ensuring agreement with experimental data. A decrease in θ_s by a factor of 10 is accompanied by a twofold increase in E_{out} relative to the data in Fig. 5. At $\theta_s = 0$, E_{out} increases by an additional 15%. This is not surprising because the nonsaturable loss θ_s in the laser under consideration is about a factor of 2.5 smaller than the loss due to the mirror ($R = 0.09$ in the experiment).

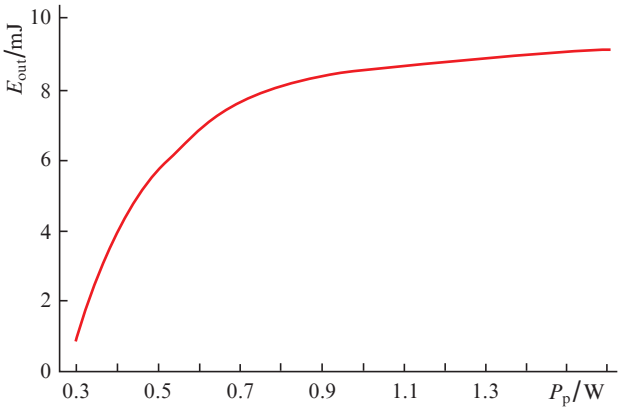

Figure 5. Output pulse energy as a function of pump power.

5. Discussion

The good agreement between the calculation results and experimental data [14] allows output characteristics of the laser under consideration to be predicted with a reasonable probability for another set of its parameters. Since the most important parameter is the output power P_{out}, we performed a series of calculations to assess how the reflectivity of the mirror (R) and the geometric dimensions L_1 and L_2 influence P_{out}. The parameters of the gain medium were fixed in the calculations, and the pump power was constant at 1 W. For comparison, Fig. 6a shows previous results and Figs 6b and 6c show calculation results for other values of R, L_1, and L_2 (indicated at the right of each panel). In calculating P_{out} (Fig. 6c), the ratio of the fractional pump powers for the oscillator and amplifier was taken to be equal to the ratio of the lengths of the corresponding fibre sections. The other numbers in Fig. 6 indicate the time of each pulse.

All other calculation parameters being constant, $R = 0.32$ was found to be an optimal value. It is seen from Fig. 6b that, at $R = 0.32$, the structure of the pulses is shifted to shorter τ by unity and the peak power of the highest pulse is approximately twice that at $R = 0.09$ in experiments. Varying the ratio of the lengths of the oscillator and amplifier sections also changes the time shift, but at $R = 0.32$ the output power rises only slightly (Fig. 6c). These calculations demonstrate that, to maximise P_{out} at a given P_p, one should jointly optimise the parameter R and the ratio of the oscillator and amplifier lengths.

In discussing the present results, it is worth noting that a multipeak structure of output light in the case of Q-switching was studied numerically in other fibre lasers. For example, Adachi and Koyamada [7] reported data on such structures in gain media of various lengths under various modulator operation conditions for an erbium-doped fibre ring laser. They concluded that a structure with narrow peaks emerged

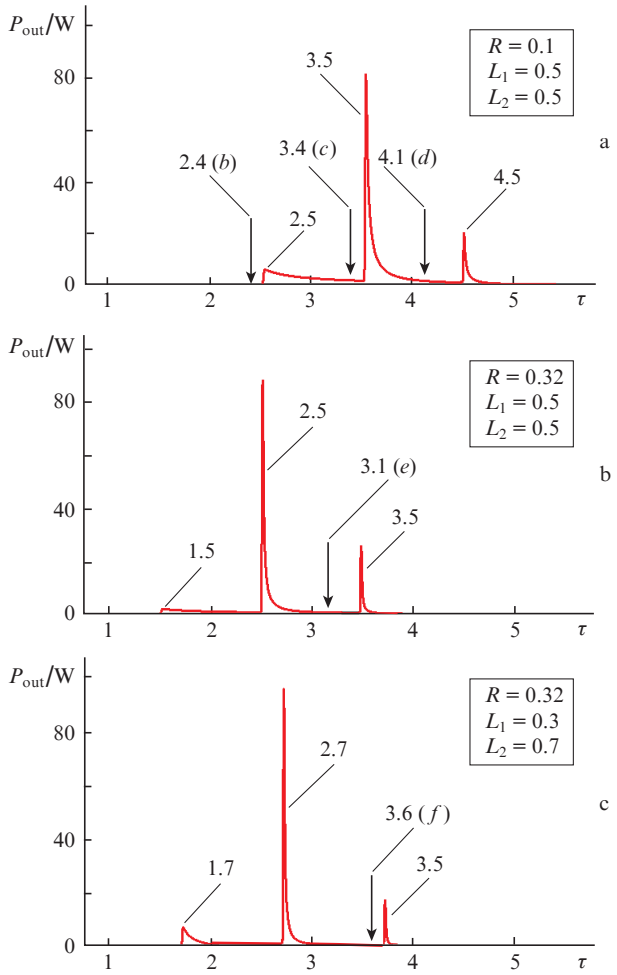

Figure 6. Laser output power calculated for different parameters. Time zero represents the instant at which the modulator was opened.

if the modulator was turned on for a sufficiently short time τ_q (shorter than the cavity round-trip time τ_c). In particular, at $\tau_c \approx 500$ ns, $\tau_q = 0.2\tau_c$, and a laser gain medium length of 120 m, the width of an individual peak was $\sim 0.2\tau_c$. The formation of a series of peaks was attributed to inversion depletion. Wang and Xu [8, 9] studied a multipeak structure in linear and ring configurations of a double-clad ytterbium-doped fibre laser. In the case of a 15-m-long linear fibre, an AOM with an additional, highly reflective mirror was used as a modulator. When the modulator was closed, it did not reflect incident light. After opening the modulator (first order of diffraction from the mirror), reflectivity was $R \sim 0.9$. On the other side of the cavity, a Bragg mirror with 20% reflectivity was placed. They examined the feasibility of controlling the spike structure of output light in the forward and backward directions by varying the AOM turning-on time and the evolution of the structures after subsequent turning-ons. In most cases, output light had the form of several pulses with a smooth power profile, separated by intervals with a nonzero intensity. It was concluded that the spike structure was a consequence of an amplified spontaneous emission wave that resulted from Q-factor modulation and that its distinctive features depended on the modulator turning-on time and the state of the medium.

Note that the conclusion as to the formation of a spike structure was typically drawn from analysis of output light characteristics. For this reason, relations between such characteristics and parameters of the gain medium remained unclear, even though there was substantial evidence of such relations. For example, dynamics of a nonuniform gain distribution in the medium were left out of account, which made it impossible to understand why there was only a small number of pulses with different amplitudes. This led us to expend considerable effort in order to gain detailed insight into the nature of the formation of output light of a Q-switched bismuth fibre laser by analysing the dynamics of the distributions of the main laser parameters along the active fibre. In those calculations, we assumed that, in all cases, the modulator was opened sufficiently rapidly: in 20 ns.

Figure 7 illustrates the development of laser pulses at different instants in time at constant pump power of 1 W and $R = 0.1$. The instants of time indicated in Fig. 7 (except Fig. 7a) are marked by vertical arrows in Fig. 6a. Figure 7a shows distributions just $\tau = 0.1$ after the modulator was opened. During this short time, neither the w_p^+ or w_p^- pump wave intensity distribution nor the gain coefficient (α) distribution undergoes any noticeable changes relative to steady-state distributions with the modulator closed and remain symmetric with respect to the centre, where the modulator is located. The fibre absorbs about 80% of the pump power. The gain coefficient α is the largest throughout the active fibre and, at the pump power in question, exceeds the loss θ_s by a factor of 5.2. It is seen that, in both directions from the modulator, two broadband ASE components and a signal wave begin to propagate. As would be expected, the ASE intensity is higher. The travelling wave edge width corresponds to the modulator turning-on time, and in this stage none of the waves saturates the gain medium.

The w_s^+ intensity of the waves that leave the gain medium at a time $\tau = 0.5$ and 1.5 remains low and is not seen in Fig. 6a. In the range $\tau = 0.5$ to 2, the signal wave, which partially returns to the gain medium, is amplified much more rapidly than the waves of the broadband ASE components. This leads to drastic changes in the relationship between the intensities of the signal wave and the ASE waves: the intensity of these latter at a time $\tau = 2$ proves to be negligible. The saturation of the medium with the signal wave gradually increases.

The distributions shown in Fig. 7b refer to a time $\tau = 2.4$, when the first sufficiently intense signal wave pulse, which caused noticeable saturation of the gain medium, approaches the mirror ($x = 1$). It is seen that the peak intensity of this pulse exceeds that at a time $\tau = 0.1$ (Fig. 7a) by 10^5 times. At this instant in time, the active medium, especially that in the amplifier, has a marked gain (α) saturation, which leads to symmetry distortion of the $w_p^{\pm}$ distributions. At the same time, it follows from Fig. 7b that, abandoning the active zone, a pulse leaves a sufficiently large gain reserve. For this reason, passing another round trip, the part of the pulse reflected from the mirror forms one or a few more output pulses. The result is a multipeak lasing structure.

Figure 7c shows the distributions at an instant in time preceding the exit of the strongest (second) pulse from the amplifier. As follows from Fig. 7c, the propagation of this pulse in the gain medium effectively saturates the gain in the amplifier, where its intensity is highest. As a result of the saturation, the edge and pulse widths decrease because the leading pulse edge travels through a weakly saturated medium, whereas the rest of the pulse travels through a saturated one. Note that, at the trailing edge, the medium becomes absorbing because the

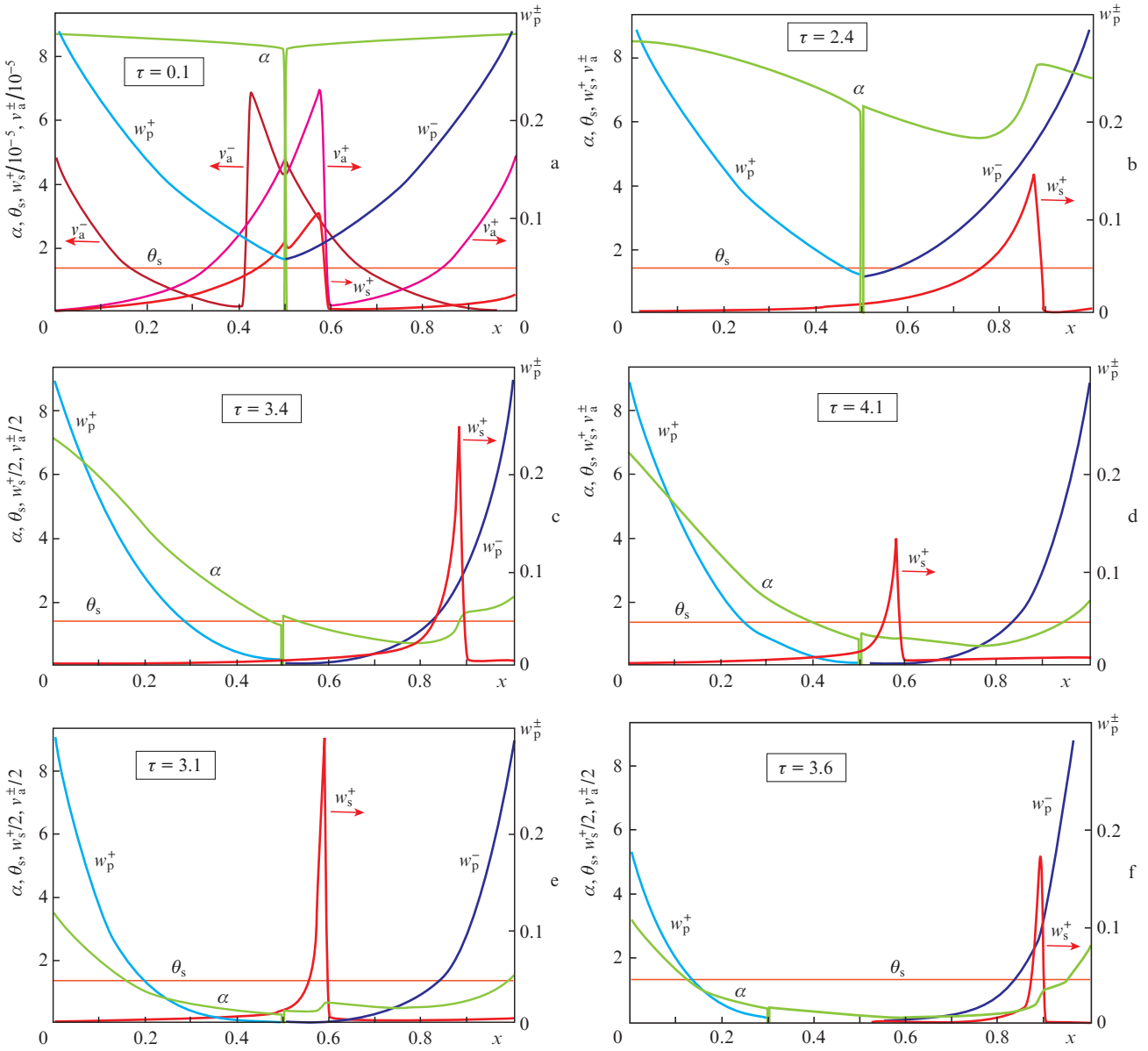

Figure 7. (Colour online) $w_p^{\pm}$ pump intensity, w_s^+ lasing signal, v_a^+ and v_a^- ASE wave intensity, α gain coefficient, and θ_s loss distributions along the cavity at different instants in time.

nonsaturable loss θ_s exceeds the saturated gain. Comparison of the α distributions in the amplifier in Figs 7b and 7c demonstrates that the curves differ in behaviour in a small region near $x = 1$, where the gain drops in the former case and rises in the latter. The reason for this is that, in the former case, the saturation caused by the preceding pulses is rather weak and is relatively slowly compensated for by pumping (at $x = 1$, the pump intensity is highest). In the latter case, there is strong saturation, and pumping in this region of the medium has a noticeable effect over a time of unity.

Figure 7d illustrates the formation of a third pulse, which has the smallest amplitude. After partial reflection of the second pulse from the mirror, the third pulse is amplified in the oscillator to an amplitude comparable to that of the preceding pulse (time $\tau = 4.1$). At the same time, in the rest of the path to the cavity output (which takes a time of 0.4) the third pulse travels through an absorbing medium, so it is not surprising that the pulse emerging from the amplifier has a small amplitude (Fig. 6a). It is seen from Fig. 7d that, after the exit of the third pulse, there is a gain left in the medium, concentrated in the oscillator. This suggests the feasibility of improving the efficiency of the laser, as mentioned above.

The salient features of pulse formation at reflectivity R increased to 0.32 can be seen in Fig. 7e. The increase in reflectivity leads to an increase in w_s^+ intensity and a stronger saturation of the medium by a pulse with the highest power (exit at $\tau = 2.5$). The next pulse (exit at $\tau = 3.5$), whose formation is shown in Fig. 7e, can be amplified only in the oscillator region and subsequently, after traversing the amplifier with absorption, will be severely attenuated. Note that further increase in R and the corresponding rise in w_s^+ do not lead to any increase in output intensity because this is accompanied by a decrease in the fraction of w_s^+ that leaves the gain medium.

The distributions shown in Fig. 7f were obtained for a laser configuration with asymmetric excitation: $L_1 : L_2 =$

0.3 : 0.7 and $R = 0.32$. Since the pump power is distributed between the oscillator and amplifier in the same ratio, the oscillator is too 'weak'. Because of this, the gain in the oscillator cannot be considerably reduced, and the gain in the nearest part of the amplifier remains positive after the second pulse. Nevertheless, it follows from comparison with the data in Fig. 7c that the 'residual' gain is lower in this case. The small increase in the output pulse amplitude is due to the larger length of the amplifier, in which w_s^+ pulse steepening occurs.

Note that, in a sufficiently long cavity, where with increasing pump power the rise in output power is limited, in particular, due to the effect of the nonsaturable loss, the optimisation of laser parameters plays an increased role. The present calculation results demonstrate that the output pulse amplitude can be increased by jointly optimising the geometric parameters and reflectivity of the mirror. It seems likely that the parameters to be optimised can include the length of the gain medium and the pump power distribution between the parts of the gain medium. Output characteristics can then be improved as a result of multifactorial optimisation. For this purpose, it is also reasonable to design other functional configurations of bismuth-doped fibre lasers.

6. Conclusions

The proposed model for a bismuth-doped fibre ring laser has been shown to adequately describe a considerable amount of experimental data. This allows simulation results to be considered reliable and makes it possible to understand and scrutinise those laser characteristics defying a detailed experimental analysis. In particular, it has been shown that multipeak lasing and complex-shaped pulse generation are due to incomplete saturation of the gain medium. In the laser configuration examined, changes in the initial spontaneous emission intensity have a weak effect on the output pulse amplitude. Simulation results help understand how the pulse amplitude and width vary in the case of a gain medium with a highly nonuniform pumping and gain. We have demonstrated that, by varying some parameters, the output pulse amplitude in the model laser can be increased at least twofold.

References

1. Firstova E.G., Bufetov I.A., Khopin V.F., et al. *Quantum Electron*., **45** (1), 59 (2015) [*Kvantovaya Elektron*., **45** (1), 59 (2015)].
2. Thipparapu N.K., Wang Y., Wang S., et al. *Opt. Mater. Express*, **9** (6), 2446 (2019).
3. Bufetov I.A., Melkumov M.A., Firstov S.V., et al. *IEEE J. Sel. Top. Quantum Electron*., **20** (5), 111 (2014).
4. Gumenyuk R., Puustinen J., Shubin A.V., et al. *Opt. Lett*., **38** (20), 4005 (2013).
5. Khegai A.M., Afanas'ev F.V., Riumkin K.E., et al. *Quantum Electron*., **46** (12), 1077 (2016) [*Kvantovaya Elektron*., **46** (12), 1077 (2016)].
6. Khegai A., Melkumov M., Firstov S., et al. *Opt. Express*, **26** (18), 23911 (2018).
7. Adachi S., Koyamada Y. *J. Lightwave Technol*., **20** (8), 1506 (2002).
8. Wang Y., Xu C.-Q. *Opt. Lett*., **29** (10), 1060 (2004).
9. Wang Y., Xu C.-Q. *Prog. Quantum Electron*., **31**, 31 (2007).
10. Wang Y., Martinez-Rios A., Po H. *Opt. Commun*., **224**, 113 (2003).
11. Roy P., Pagnoux D. *Opt. Fiber Technol*., **2**, 235 (1996).
12. Jung M., Melkumov M., Khopin V.F., et al. *Laser Phys. Lett*., **10** (12), 125104 (2013).
13. Jung M., Melkumov M., Khopin V.F., et al. *Laser Phys. Lett*., **11**, 125102 (2014).
14. Khegai A., Firstov S., Riumkin K., et al. *IEEE Photonics Technol. Lett*., **31** (12), 963 (2019).
15. Kowalski F.V., Shattil S.J., Hale P.D. *Appl. Phys. Lett*., **53**, 734 (1988).
16. Littler I.C.M., Balle S., Bergmann K. *J. Opt. Soc. Am. B*, **8** (7), 1412 (1991).